`carlomat_3.0,`

an automatic tool for the electron–positron annihilation into hadrons at low energies

Karol Kołodziej[1]

Institute of Physics, University of Silesia
ul. Uniwersytecka 4, PL-40007 Katowice, Poland

Abstract

A new version of `carlomat` that allows to generate automatically the Monte Carlo programs dedicated to the description of the processes $e^+e^- \to$ hadrons at low center-of-mass energies is presented. The program has been substantially modified in order to incorporate the photon–vector meson mixing terms and to make possible computation of the helicity amplitudes involving the Feynman interaction vertices of new tensor structures, like those predicted by the Resonance Chiral Theory or Hidden Local Symmetry model, and the effective Lagrangian of the electromagnetic interaction of the nucleons. Moreover, a number of new options have been introduced in the program in order to enable a better control over the effective models implemented. In particular, they offer a possibility to determine the dominant production mechanisms of the final state chosen by the user.

---

[1]E-mail: karol.kolodziej@us.edu.pl

PROGRAM SUMMARY

Program title: `carlomat, version 3.0`
Catalogue identifier:
Program summary URL:
Program obtainable from: CPC Program Library, Queen's University, Belfast, N. Ireland
Licensing provisions: Standard CPC licence
No. of lines in distributed program, including test data, etc.:
No. of bytes in distributed program, including test data, etc.:
Distribution format: tar.gz
Programming language: `Fortran 90/95`
Computer: All
Operating system: Linux
Classification:
Nature of problem:
Predictions for reactions of low energy e^+e^--annihilation into final states containing pions, kaons, light vector mesons, one or more photons and light fermion pairs within the Standard Model and effective models inspired by the Resonance Chiral Theory or Hidden Local Symmetry model. Description of the electromagnetic production of nucleon pairs within the effective Lagrangian approach.
Solution method:
As in former versions, a program for the Monte Carlo (MC) simulation of $e^+e^- \rightarrow$ hadrons at low energies is generated in a fully automatic way for a user specified process. However, the user is supposed to select a number of options and adjust arbitrary parameters in the main part of the MC computation program in order to obtain possibly the best description of experimental data. To this end, the user can also easily supplement her/his own formulae for *s*-dependent vector meson widths or running couplings by appropriately modifying corresponding subroutines.
Reasons for new version:
Processes of $e^+e^- \rightarrow$ hadrons in the energy range below the J/ψ threshold cannot be described in the framework of perturbative quantum chromodynamics. The scalar electrodynamics which has been implemented in `carlomat_2.0` [1] does not provide a satisfactory description either. The most promising theoretical frameworks in this context are the Resonance Chiral Theory or Hidden Local Symmetry model which, among others, involve the photon–vector meson mixing and a number of vertices of rather complicated Lorentz tensor structure that is not present in the Standard Model or scalar QED. Already at low energies, the hadronic final states may consist of several particles, such as pions, kaons, or nucleons which can be accompanied by one or more photons, or light fermion pairs such as e^+e^-, or $\mu^+\mu^-$. The number of Feynman diagrams of such multiparticle reactions grows substantially with increasing numbers of interaction vertices and mixing terms of the effective models. Therefore, it is highly desirable to automatize the calculations. At the same time, new

program options should provide the user with an easy way of implementing her/his own changes in the program in order to better fit the experimental data.

Summary of revisions:

The code-generation part of the program has been substantially modified in order to incorporate the photon–vector meson mixing and calls to new subroutines for computation of the helicity amplitudes of the building blocks and complete Feynman diagrams which contain new interaction vertices and mixing terms. The subroutine library of `carlomat` has been extended to make possible computation of the helicity amplitudes involving the Feynman interaction vertices of new Lorentz tensor structures. Many subroutines have been modified in order to incorporate the q^2-dependent couplings and vector meson widths. A number of options have been introduced in order to give a better control of the effective model implemented.

Restrictions:

As in previous versions of the program the number of particles is limited to 12 which exceeds typical numbers of particles of the exclusive low energy e^+e^--annihilation processes. However, in the presence of photon–vector meson mixing, the Feynman diagrams proliferate, for example, with currently implemented Feynman rules, there are 90672 diagrams of $e^+e^- \to 3(\pi^+\pi^-)$. Hence, the compilation time of generated code may become very long already for processes with smaller number of the final state particles. Many couplings of the effective models are not known with good enough precision and must be adjusted in consecutive runs of the program in order to obtain satisfactory description of the experimental data.

Running time:

Depends on the selected process. Typical running time for the code generation vary from a fraction of a second for, e.g., $e^+e^- \to \pi^+\pi^-K^+K^-$ to about 2 minutes for $e^+e^- \to 3(\pi^+\pi^-)$. It may become substantially longer for processes with more particles in the final state. The execution time necessary to produce the appended test output files for $e^+e^- \to \pi^+\pi^-\mu^+\mu^-\gamma$ and $e^+e^- \to \pi^+\pi^-\pi^+\pi^-\gamma$ was 13s and 4s, respectively. The code generation for both processes took a fraction of a second time for each process.

1 Introduction

Hadronic contributions to the vacuum polarization are the major factor that influences precision of theoretical predictions for the muon anomaly a_μ and plays an important role in the evolution of the fine structure constant $\alpha(Q^2)$ from the Thomson limit to high energy scales. Improving the precision of predictions for the muon anomaly becomes vital in the prospect of forthcoming measurements in Fermilab that should reduce the experimental error of a_μ to 0.14 parts per million, while the better

precision of $\alpha(m_Z^2)$ would be important for the precision data analysis from the future high energy e^+e^- collider, which would most probably include a giga-Z option. Because of the breakdown of predictive power of the perturbative QCD at low momentum transfer, the hadronic contributions to the vacuum polarization are determined, with the help of dispersion relations, from the energy dependence of the total cross section of electron–positron annihilation into hadrons, $\sigma_{e^+e^-\to\text{hadrons}}(s)$. Below the J/ψ production threshold, $\sigma_{e^+e^-\to\text{hadrons}}$ must be measured and confronted with theoretical predictions of some effective model for the low energy hadron physics.

There are two QCD inspired theoretical frameworks which seem to be applicable in this context: the Resonance Chiral Theory (RχT) [2] and the Hidden Local Symmetry (HLS) model [3], which were proven to be essentially equivalent [4]. For example, the HLS model allowed for a quite satisfactory simultaneous description of most hadronic e^+e^--annihilation channels in the low energy range, including ϕ-resonance and 10 decay widths, mostly radiative ones, of light mesons and allowed to resolve the inconsistency between the e^+e^--annihilation to $\pi^+\pi^-$ and the $\tau^\pm$-decay to $\pi^\pm\pi^0\nu_\tau$ [5], [6]. The hadronic currents based on RχT were implemented in TAUOLA, a τ-decay Monte Carlo (MC) generator [7], and used for description of the τ lepton decay into two or three pseudoscalar mesons that constitute 88% of the τ hadronic decay width in Ref. [8] and later improved for $\tau^\pm \to \pi^\pm\pi^\pm\pi^\mp\nu_\tau$ decay mode in Ref. [9] which allowed to successfully model the one-dimensional distributions measured by the BaBar collaboration.

The number of Feynman diagrams in the framework of RχT or HLS model grows quite fast with the number of particles in the final state of $e^+e^- \to$ hadrons. In particular, in the presence of one or a few photon–vector meson mixing terms, it can easily reach a hundred thousand already for $e^+e^- \to 6\pi$. Obviously, preparation of a reliable MC generator for such a process is rather tedious a task, unless the process of code writing is fully automatized. The first step toward the automatic generation of the MC programs for description of reactions $e^+e^- \to$ hadrons was already made in carlomat_2.0 [1], in which the Feynman rules of the scalar electrodynamics (sQED) were implemented in addition to those of the Standard Model (SM). It allowed to effectively describe the electromagnetic (EM) interaction of charged pions which, at low energies, can be considered as being point like particles, see, e.g., [10]. However, the charged pion form factor that would allow to account for the bound state nature of the particle was not implemented in carlomat_2.0. In the present paper, a new version, labeled with 3.0, of a program carlomat [11], [1] is described, which to large extent should meet the requirements of automatic code generation for MC simulation of the low energetic e^+e^--annihilation into hadrons in the framework of the effective models.

The paper is organized in the following way. In Section 2, the implementation of new Feynman rules in the program is described. New options which have been implemented in the program to give the user a better control over the model are described in Section 3. Finally, the instructions for

preparation for running and usage of the program are given in Section 4.

2   New Feynman rules implemented in the program

In this section, the implementation of the Feynman rules of the HLS model that are relevant for the description of $e^+e^- \to$ hadrons in the low energy range in `carlomat_3.0` is described. Most of the rules can be derived from the Lagrangian pieces of Appendix C of Ref. [5]. The Lagrangian of EM interaction of spin 1/2 nucleons implemented in the program is described in Subsection 2.3.

2.1   Photon–vector meson mixing

The topology generator of `carlomat` takes into account only triple and quartic vertices, therefore the mixing should be added in subroutine `checktop`, where topologies of diagrams are confronted with the implemented Feynman rules. The procedure was described in detail in Ref. [11]. For the sake of clarity let us remind here, that every topology in `carlomat` is divided into two parts, each being checked against the Feynman rules separately. This is done by consecutive calls to subroutine `genpart` that combines two (three) particles into the third (fourth) leg of a triple (quartic) Feynman vertex which is then folded with the adjacent Feynman propagator to form an off-shell particle. The latter is represented by an array of spinors, polarization vectors or scalars, whose elements are labeled with different combinations of the polarization indices of the particle spinors or polarization vectors of which they are formed. At this point, if the particle mixing is present, a new subroutine `mixpl` is called to check whether the propagator of the off-shell particle can be mixed with some other propagator or not, if so, a new off-shell particle is formed. The particle with mixing is appropriately tagged in order not to be mixed again, because, according to Fig. 1, the mixing term contains an extra power of the electric charge e and therefore should be considered as the next to leading-order correction. This procedure is being repeated until finally two off-shell particles are formed, corresponding to both parts of the considered topology. Then, a modified subroutine `matchkk` is called which checks, whether the particles can be matched in the Feynman diagram with the Feynman propagator or, if none of them has been mixed yet, with some of the mixing terms of Fig. 1.

In spite of being conceptually quite simple, the implementation of particle mixing required substantial changes in the code-generation part of the program. Moreover, new subroutines `bbkk` and `bbmd` have been written to compute, respectively, the polarization vectors of the off-shell particle and

helicity amplitudes of the Feynman diagrams in the case of mixing.

$$A^\mu(q) \qquad V^\nu(q)$$

$$\equiv \quad -e f_{AV}(q^2)\, g^{\mu\nu}, \quad \text{with} \quad V = \rho^0, \omega, \phi, \rho_1, \rho_2.$$

Figure 1: The photon–vector meson mixing diagrams implemented in the current version of the program; ρ_1 and ρ_2 stand for $\rho(1450)$ and $\rho(1700)$, respectively.

2.2 Interaction vertices

The triple and quartic interaction vertices of the HLS model that are implemented in `carlomat_3.0` are depicted in Figs. 2–4, where all the particle four momenta are assumed to be incoming to the vertex and $\varepsilon^{\mu\nu\rho\sigma}$, with $\varepsilon^{0123} = 1$, is the totally antisymmetric Levi-Civita tensor. A number of new subroutines for computation of the building blocks and complete amplitudes of the Feynman diagrams containing vertices of new tensor structure have been written. The implementation of calls to the new subroutines required some changes in the code-generation part of the program which concerned mainly subroutine `genpart`.

The triple vertices of the photon A^μ or vector meson V^μ interaction with the pseudoscalar meson pair $P\bar{P}$ which have the form similar to the triple vertex of sQED are shown in Fig. 2. The only difference is the replacement

$$e \rightarrow e f_{APP}(q^2) \qquad \text{and} \qquad e \rightarrow f_{VPP}(q^2), \tag{1}$$

where $V = \rho^0, \omega, \phi, \rho_1, \rho_2$ and $P = \pi^+, K^+, K^0$. Although couplings of $\rho_1 = \rho(1450)$ and $\rho_2 = \rho(1700)$ to other particles are hard to define on the basis of existing data [12], the interaction vertices $\rho_i \pi^+ \pi^-$ and mixing terms $\gamma - \rho_i$, $i = 1, 2$, have been included in the program just to enable tests of their possible influence on some observables, e.g., on the pion form factor, where they play a role.

Subroutines `ppakk`, `appkk` and `papkk` for the computation of building blocks of the Feynman diagrams, and `ppamd`, `appmd` and `papmd` for the computation of the helicity amplitudes in the sQED of `carlomat_2.0` have been all supplemented with an option `ig`, which allows to take into account the q^2-dependent couplings of (1). Subroutines `ppakk` and `ppamd` have been additionally supplied with an option `iwdth`, that gives a possibility to include the s-dependent width of a vector meson. The use of both options is explained in Section 3.

Triple interaction vertices of the HLS model that have a form different from that of the triple vertices of the SM or sQED are depicted in Fig. 3. New subroutines that have been written in order to
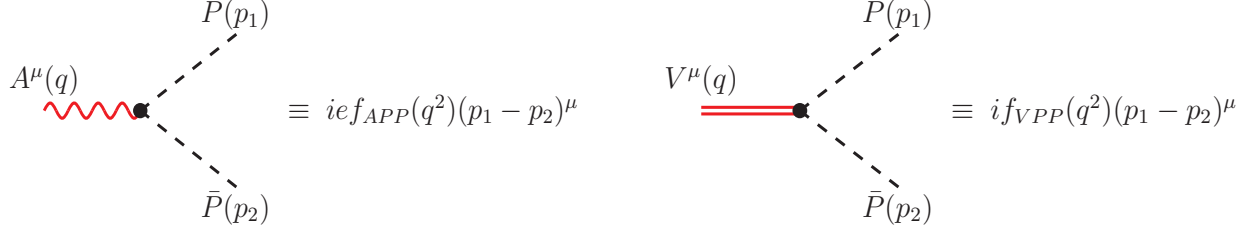
Figure 2: Triple vertices of the photon A^μ or vector meson V^μ, $V = \rho^0, \omega, \phi$, interaction with the pseudoscalar meson pair $P\bar{P}$, $P = \pi^+, K^+, K^0$, of the same form as that of the triple vertex of sQED.
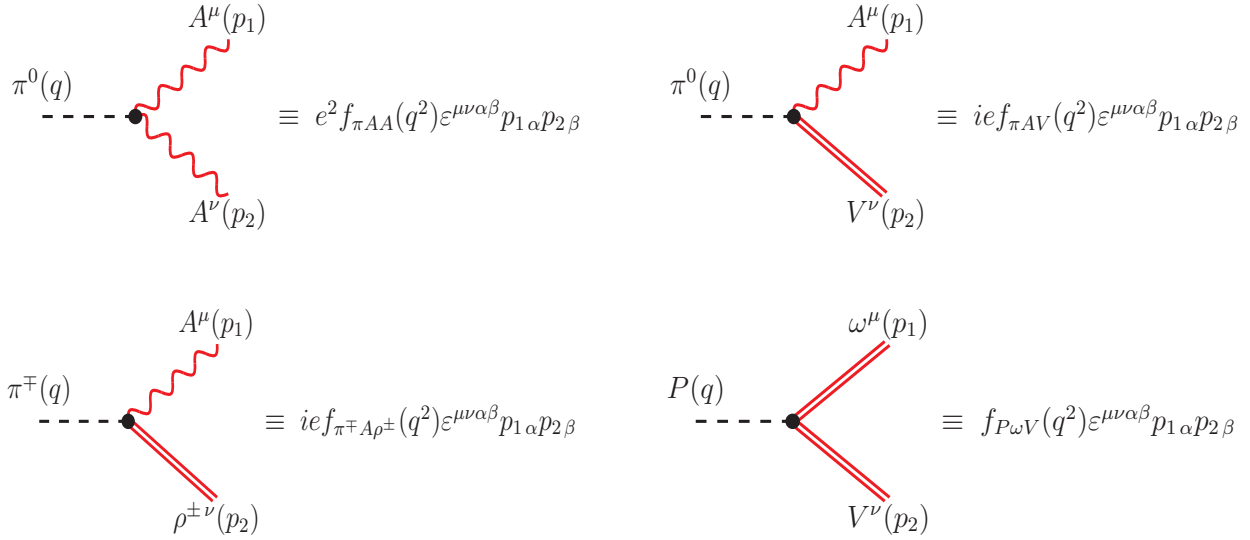

Figure 3: Triple vertices of the pion interaction with photons or vector mesons, where, in the top right corner, $V = \rho^0, \omega$, in the bottom right corner $P = \pi^0$ and $V = \rho^0$ or $P = \pi^\mp$ and $V = \rho^\pm$.

compute the corresponding building blocks and helicity amplitudes are: `pvvkk`, `pvvmd`, `vvpkk` and `vvpmd`. All of them include the running-coupling option `ig`, and the first one, whose output is an array of four vectors corresponding to all possible helicities of the scalar and vector particles they are composed of, includes in addition the running-width option `iwdth`.

The quartic interaction vertices of the HLS model implemented in the current version of the program are shown in Fig. 4. The vertices in the first row have the same tensor form as the quartic vertex of the sQED or the quartic vertices of the Nambu-Goldstone boson – gauge boson interaction of the SM, which have been implemented already in the first version of `carlomat`. Hence, the corresponding building blocks and helicity amplitudes can be computed with modified subroutines `vvsskk`,
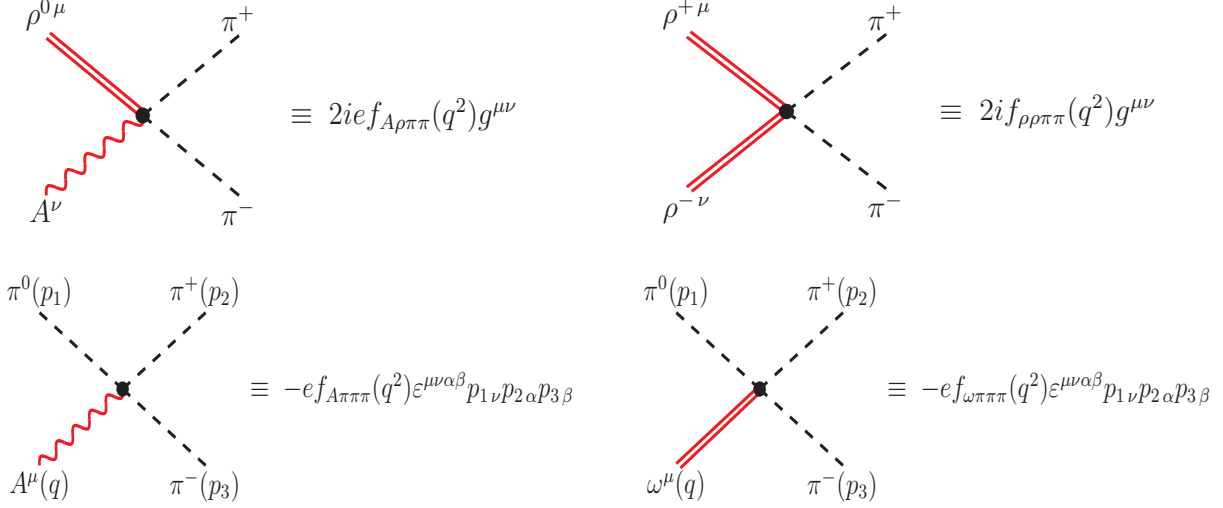
Figure 4: Quartic vertices of the HLS model implemented in the current version of the program. The quartic vertex $AA\pi^+\pi^-$ of sQED, implemented already in `carlomat_2.0`, is not shown.

`vvssmd`, `vsvskk`, `vsvsmd`, `vssvkk`, `vssvmd`, `svvskk`, `svvsmd`, `ssvvkk`, `ssvvmd`, `svsvkk` and `svsvmd`, which have been all supplied with the running-coupling option `ig`. Subroutines `vssvkk`, `ssvvkk` and `svsvkk` have been moreover supplemented with the running-width option `iwidth`. The tensor form of the vertices in the second row of Fig. 4 is different. Therefore, the corresponding building blocks and helicity amplitudes are computed with newly written subroutines `pppvkk`, `pppvmd`, `vpppkk` and `vpppmd`.

2.3 Electromagnetic interaction of nucleons

The Lagrangian of EM interaction of spin 1/2 nucleons has the following form:

$$\mathcal{L}_{ANN} = eA_\mu \bar{N}(p') \left[\gamma^\mu F_1(Q^2) + \frac{i}{2m_N} \sigma^{\mu\nu} q_\nu F_2(Q^2) \right] N(p), \qquad (2)$$

where $\sigma^{\mu\nu} = \frac{i}{2}[\gamma^\mu, \gamma^\nu]$, with γ^μ, $\mu = 0, 1, 2, 3$, being the Dirac matrices, $q = p - p'$ is the four momentum transfer, $F_1(Q^2)$ and $F_2(Q^2)$ are the form factors and $Q^2 = -q^2$. The form of Eq. (2) is similar to that of the effective Lagrangian of the Wtb interaction given by Eq. (4) of Ref. [1]. Due to this fact, the implementation of the corresponding Feynman rules for the nucleon–photon interaction was straightforward. To compute the corresponding building blocks and helicity amplitudes the following new subroutines have been written: `annkk`, `annmd`, `nnakk`, `nnamd`, `nankk` and `nanmd`

and the calls to them have been appropriately implemented in subroutine `genpart`. The form factors $F_1(Q^2)$ and $F_2(Q^2)$ have been adopted from `PHOKARA` [13] with the help of an interface subroutine `nuclff_phok`. In this way, the MC simulations of processes involving the EM production of the nucleon pairs have become possible.

3 New program options

New options which have been added in the program to give the user a better control over the implemented models for the description of the electron–positron annihilation into hadrons at low energies are explained below.

All subroutines that are used to compute the building blocks or the complete helicity amplitudes of the Feynman diagrams of Figs. 2–4 have been supplied with the running-coupling option the name of which is formed by adding a prefix `i` to the name of the corresponding coupling, as the name is created in exactly the same way at the stage of code generation. The options are to be specified in subroutine `couplsm`, where they are defined below the assignment instruction for each particular coupling.

   `icoupl_name=0/1,2,...`   if the `fixed`/`running` coupling is to be used in the computation,

where choices `1,2,...` corresponding to different running couplings $f_{...}(q^2)$ of Figs. 1–4 should be added by the user as extra `else if (ig == ...)` `then` blocks in subroutine `runcoupl`. The block must contain an assignment for a double complex variable `rg` in terms of the four momentum transfer squared q^2 and any other physical parameters that are available in module `inprms`. The actual form of the four momentum transfer q is determined automatically from the four momentum conservation in the corresponding interaction vertex at the stage of code generation. Many couplings of the RχT or HLS model are not known well enough and therefore must be adjusted in consecutive runs of the program in order to obtain satisfactory description of the experimental data. If there are no hints as to the form of the running couplings $f_{...}(q^2)$ then it is recommended to set the corresponding running-coupling option to 0, which means that the fixed coupling is to be used in the computation. The user can also modify any of the fixed couplings by changing the corresponding assignments in `couplsm`, where the couplings are defined in terms of the physical parameters of module `inprms`.

The subroutines for computation of the four vectors representing vector mesons have been in addition supplied with the running-width option `iwdth_name`, i.e. `igmrh`, `igmom`, `igmph`, `igmr1`, `igmr2` for the running width of $\rho^0, \omega, \phi, \rho_1, \rho_2$, respectively:

`iwdth_name=0/1,2,3` if the `fixed/running` width of the vector particle should be used,

where choices 1,2,3 refer to different running-width options in subroutine `runwidth` which again can easily be extended by the user. The options are controlled from `carlocom`, the main part of the MC computation program.

The main part of the MC computation program `carlocom` contains a few flags: `iarho`, `iaome`, `iaphi`, `iarho1` and `iarho2` that allow to switch off and on the photon mixing with ρ, ω, ϕ, ρ_1 and ρ_2 vector mesons without a need of running the code-generation program anew, provided that the corresponding mixing terms were included in a file `vertices.dat` when the MC code was generated. This gives a possibility to determine the dominant production mechanisms of the final state considered by the user.

In order to give a better control over the mixing contributions to a given process, subroutines `bbkk` and `bbmd` are equipped with the option:

`iwgt=0/1,2,...` if the additional complex factor $c_1, c_2, ...$ is `not/is` to be included in $f_{AV}(q^2)$ of Fig. 1, i.e. in the amplitude of the Feynman diagrams containing this particular particle mixing contribution.

The actual names for that option in `carlocom` are: `imrho`, `imome`, `imphi`, `imrh1`, `imrh2` for the $\rho^0, \omega, \phi, \rho_1, \rho_2$ meson, respectively. The complex factor c_j, $j = 1, 2, ...$ is given by

$$c_j = w_j \, e^{i\varphi_j} f_j(q^2), \tag{3}$$

where w_j is a positive weight, φ_j is an angle in degrees, which should be both specified for each possible particle mixing term in the main program for the MC computation `carlocom`, and $f_j(q^2)$ is a possible four momentum transfer dependence that is defined in subroutine `weightfactor`. Actually only three simple dependences corresponding to `iwgt=1,2,3` are currently defined in `weightfactor`, but the user can easily add more options by implementing new `else if (iwgt == ...)` then conditions.

An important new option in the program, which allows to test the EM gauge invariance for processes with one or more external photons, is `igauge` in `carlocom.f`:

`igauge=1,2,.../else` if the gauge invariance `is/is not` to be tested,

where 1,2,... is the number of a photon, counting from left to right, whose polarization four vector is replaced with its four momentum.

To illustrate how this option can be used in practice, consider the following radiative processes:

$$e^+e^- \rightarrow \pi^+\pi^-\mu^+\mu^-\gamma, \tag{4}$$
$$e^+e^- \rightarrow \pi^+\pi^-\pi^+\pi^-\gamma. \tag{5}$$

Taking into account the Feynman rules of SM, without the Higgs couplings to electrons and muons, sQED, the $\gamma - \rho^0$ mixing of Fig. 1 and the vertices: $\gamma\pi^+\pi^-$ and $\rho^0\pi^+\pi^-$ of Fig. 2, $\pi^0\gamma\gamma$ and $\pi^0\gamma\rho^0$ of Fig. 3 and $\gamma\rho^0\pi^+\pi^-$ and $\gamma\pi^0\pi^+\pi^-$ of Fig. 4, processes (4) and (5) receive contribution from, respectively, 209 and 774 Feynman diagrams. If, in addition, the vertices $\pi^\mp\gamma\rho^\pm$ of Fig. 3 are included then the number of diagrams of processes (4) and (5) grows, respectively, to 231 and 968. The cross sections of processes (4) and (5) at $\sqrt{s} = 1$ GeV, with the following cuts on the angles between the photon and a lepton $\theta_{\gamma l}$, the photon and a pion $\theta_{\pi l}$ and the photon energy:

$$\theta_{\gamma l} > 5°, \qquad \theta_{\gamma\pi} > 5°, \qquad E_\gamma > 10 \,\text{MeV}, \tag{6}$$

are presented in Table 1. The cross sections without (with) contribution from the $\pi^\mp\gamma\rho^\pm$ interaction vertices of Fig. 3 are printed in the first (second) column for each process. If `igauge=1` then the cross section drops by about 32 orders of magnitude, which means that the EM gauge invariance works perfectly well. However, if the vertices $\pi^\mp\gamma\rho^\pm$ of Fig. 3 are included then the EM gauge invariance is not so perfect any more. For process (4) this is caused by the two Feynman diagrams depicted in Fig. 5. To justify this statement, let us denote the four momenta of particles of process (4) by $p_1, p_2, ..., p_7$, from left to right consecutively, and consider the EM gauge invariance test for the amplitudes of the diagrams (a) and (b) of Fig. 5, which means in practice that the photon polarization four vector is replaced with its four momentum. Neglecting the i factors, which are the same for both amplitudes, and skipping polarization indices the amplitudes read:

$$
\begin{aligned}
M_a &= g^2 \varepsilon_{12\nu} \varepsilon^{\nu\mu\alpha\beta} p_{12\alpha} (-q_\beta) \frac{-g_{\mu\rho} + \frac{q_\mu q_\rho}{M^2}}{q^2 - M^2} \varepsilon_{56\sigma} \varepsilon^{\sigma\rho\gamma\delta} (-p_{56\gamma}) q_\delta s_{37} \\
&= \frac{eg^2}{q^2 - M^2} \varepsilon^{\mu\nu\alpha\beta} \varepsilon_{\mu\sigma\gamma\delta} \varepsilon_{12\nu} p_{12\alpha} p_{4\beta} \varepsilon_{56}^\sigma p_{56}^\gamma (p_3 + p_7)^\delta, \tag{7}
\end{aligned}
$$

$$
\begin{aligned}
M_b &= g^2 \varepsilon_{12\nu} \varepsilon^{\nu\mu\alpha\beta} p_{12\alpha} (-r_\beta) \frac{-g_{\mu\rho} + \frac{r_\mu r_\rho}{M^2}}{r^2 - M^2} \varepsilon_{56\sigma} \varepsilon^{\sigma\rho\gamma\delta} (-p_{56\gamma}) r_\delta s_{47} \\
&= -\frac{eg^2}{r^2 - M^2} \varepsilon^{\mu\nu\alpha\beta} \varepsilon_{\mu\sigma\gamma\delta} \varepsilon_{12\nu} p_{12\alpha} p_{3\beta} \varepsilon_{56}^\sigma p_{56}^\gamma (p_4 + p_7)^\delta, \tag{8}
\end{aligned}
$$

where ε_{12}^ν $(\varepsilon_{56}^\sigma)$ is the polarization four vector representing the $e^+e^-\gamma$ $(\mu^-\mu^+\gamma)$ vertex contracted with the adjacent photon propagator, $M^2 = m_\rho^2 - im_\rho\Gamma_\rho$ is the complex ρ meson mass parameter, $p_{12} = p_1 + p_2$, $p_{56} = p_5 + p_6$, $q = p_{56} + p_3 + p_7$ and $r = p_{56} + p_4 + p_7$ are four momenta of intermediate

11

virtual photons and $\rho^{\pm}$ mesons, and the coupling $g = e f_{\pi^- A \rho^+}(q^2) = e f_{\pi^+ A \rho^-}(q^2) = e f_{\pi^- A \rho^+}(r^2) = e f_{\pi^+ A \rho^-}(r^2)$ has been assumed to have a fixed value. In the second row of Eqs. (7) and (8), use has been made of the fact that, in the EM gauge invariance test, the scalars s_{37} and s_{47} representing the $\pi^+ \pi^- \gamma$ and $\pi^- \pi^+ \gamma$ vertex multiplied with the adjacent pion propagator, take the following form:

$$s_{37} = e \frac{(p_3 + p_7 - (-p_3))^\mu \varepsilon_\mu^*(p_7)}{(p_3 + p_7)^2 - m_\pi^2}\bigg|_{\varepsilon(p_7) \to p_7} = e \frac{2 p_3 \cdot p_7}{2 p_3 \cdot p_7} = e,$$

$$s_{47} = e \frac{(-p_4 - (p_4 + p_7))^\mu \varepsilon_\mu^*(p_7)}{(p_4 + p_7)^2 - m_\pi^2}\bigg|_{\varepsilon(p_7) \to p_7} = -e \frac{2 p_4 \cdot p_7}{2 p_4 \cdot p_7} = -e.$$

It is clear from the form of Eqs. (7) and (8) that amplitudes M_a and M_b neither vanish separately nor cancel each other, contrary to the amplitudes of the other 20 Feynman diagrams of process (4) which also contain the vertices $\pi^{\mp} \gamma \rho^{\pm}$. Although that degree of gauge invariance violation should not play any role in practice, such effects should be treated with great care, as they may become sizable in some regions of the photon phase space. Therefore, it is recommended to use the `igauge` option whenever new interaction vertices are added to the program.
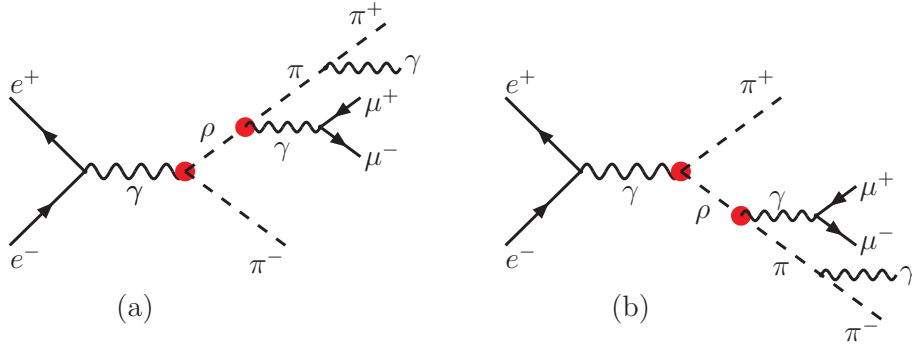

Figure 5: The Feynman diagrams of process (4) that spoil the EM gauge invariance. The blobs indicate the vertices $\pi^{\mp} \gamma \rho^{\pm}$.

4 Preparation for running and program usage

`carlomat_3.0` is distributed as a single `tar.gz` archive `carlomat_3.0.tgz` which can be downloaded from: http://kk.us.edu.pl/carlomat.html. When untared with a command
`tar -xzvf carlomat_3.0.tgz`

igauge	$\sigma(e^+e^- \to \pi^+\pi^-\pi^+\pi^-\gamma)$		$\sigma(e^+e^- \to \pi^+\pi^-\mu^+\mu^-\gamma)$	
0	11.86(5)	11.83(5)	0.0590(2)	0.0586(2)
1	0.124(2)e-30	0.441(1)e-10	0.636(9)e-33	0.973(1)e-9

Table 1: The cross sections in pb of processes (4) and (5) at $\sqrt{s} = 1$ GeV without (first column) and with (second column) contributions from the $\pi^\mp\gamma\rho^\pm$ interaction vertices of Fig. 3. The cuts used in the computation are given by (6). The numbers in parentheses show the MC uncertainty of the last decimal.

it will create directory `carlomat_3.0` with sub directories: `code_generation`, `mc_computation`, `carlolib`, `test_output` and `test_output0`.

Although `carlomat_3.0` is dedicated to the description of low energy e^+e^- scattering, interfaces to the parton density functions are kept. Therefore, files `mstwpdf.f` of MSTW [14] and `Ctq6Pdf.f` and `cteq6l.tbl` of CTEQ6 [15] are also included in the current distribution of the program, but grids must be downloaded from the web page of MSTW, see `readme` file or [1] for details. If the program will not be run for the hadron scattering processes the user can comment lines contained between `ckk_had>` and `ckk_had<` in `crosskk.f` and `parfixkk.f`, and comment or remove references to `mstw_interface.o`, `mstwpdf.o`, `Ctq6Pdf.o`, `ctq6f_interface.o` from `makefile` in `mc_computation`.

Preparation for running requires basically the same steps as in `carlomat_2.0`. They are recollected below for user's convenience.

- Choose a Fortran 90 compiler in `makefile`'s of `code_generation` and `mc_computation` and compile all the routines of `carlolib` with the same compiler as that chosen in `mc_computation`;

- Specify the process and required options in `carlomat.f` and execute `make code` from the command line in `code_generation`;

- Go to `mc_computation`, choose the center of mass energy and required options in `carlocom.f` and execute `make mc` in the command line.

Whenever the Fortran compiler is changed, or a compiled program is transferred to another computer with a different processor, all the object and module files should be deleted by executing the commands:
`rm *.o`

```
rm *.mod
```
and the necessary steps of those listed above should be repeated.

The basic output of the MC run is written to file `tot_name`, where `name` is created automatically if the assignment for character variable
```
prcsnm='auto'
```
in `carlomat.f` is not changed to arbitrary user's defined name. The output files for processes (4) and (5) with the preselected parameters and options should reproduce those delivered in directory `test_output0`.

If the differential cross sections/distributions are required then set
```
idis=1
```
in `carlocom.f`. The number of distributions to be calculated must be specified in `distribs.f` and their parameters should be defined in `calcdis.f`. The output will be stored in data files `db#_name` and `dl#_name` which can be plotted with boxes and lines, respectively, with the use of `gnuplot`. When the run is finished all output files, except for `test` that may contain information relevant in case of unexpected program stop, are moved to directory `test_output`.

As in former versions of the program, there is a possibility of generating the unweighted events. It is governed by the option `imc` that is available in `carlocom`.

The code generation for processes (4) and (5) takes a fraction of a second time. The MC computation of the cross sections of Table 3 in 10 iterations, with a maximum of $200\,000$ calls to the integrand each, takes 142s and 43s time, respectively, for (4) and (5) on processor Intel$^{\text{R}}$ Core$^{\text{TM}}$ i5-4200M CPU @ 2.50 GHz with a 64 bit Intel Fortran compiler.

References

[1] K. Kołodziej, Comput. Phys. Commun. 185 (2014) 323.

[2] G. Ecker, J. Gasser, A. Pich, E. de Rafael, Nucl. Phys. B 321 (1989) 311.

[3] M. Bando, T. Kugo, and K. Yamawaki, Phys. Rept. 164 (1988) 217;
M. Harada and K. Yamawaki, Phys. Rept. 381 (2003) 1.

[4] G. Ecker, J. Gasser, H. Leutwyler, A. Pich, E. de Rafael, Phys. Lett. B 223 (1989) 425.

[5] M. Benayoun, P. David, L. DelBuono, F. Jegerlehner, Eur. Phys. J. C 72 (2012) 1848.

[6] M. Benayoun, P. David, L. DelBuono, F. Jegerlehner, Eur. Phys. J. C 73 (2013) 2453.

[7] S. Jadach, Z. Wąs, R. Decker, J.H. Kühn, Comput. Phys. Commun. 76 (1993) 361.

[8] O. Shekhovtsova, T. Przedziński, P. Roig, and Z. Wąs, Phys.Rev. D 86, 113008 (2012).

[9] I.M. Nugent, T. Przedziński, P. Roig, O. Shekhovtsova, Z. Wąs, Phys. Rev. D 88 (2013) 9, 093012.

[10] F. Jegerlehner, *The Anomalous Magnetic Moment of the Muon*, Springer, Nov. 2007, ISBN 9783540726333.

[11] K. Kołodziej, Comput. Phys. Commun. 180 (2009) 1671.

[12] K.A. Olive et al. (Particle Data Group), Chin. Phys. C 38 (2014) 090001.

[13] S. Tracz, H. Czyż, Acta Phys. Pol. B 44 (2013) 2281.

[14] A.D. Martin, W.J. Stirling, R. S. Thorne, G. Watt, Eur. Phys. J. C 63 (2009) 189-285.

[15] J. Pumplin et al., JHEP 07 (2002) 012.